A Hybrid Framework of Traffic Simulation and Management for Large-scale Urban Air Mobility

Canqiang Weng[a], Can Chen[a,b], Tianlu Pan[c], Renxin Zhong[a,*]

[a]*School of Intelligent Systems Engineering, Sun Yat-Sen University, Shenzhen, China*
[b]*Department of Civil and Environmental Engineering, The Hong Kong Polytechnic University, Hong Kong, China*
[c]*Department of Network Intelligence, Peng Cheng Laboratory, Shenzhen, China*

Abstract

Urban air mobility (UAM) is an emerging mode that uses low-altitude airspace to provide point-to-point air travel services. Recent advances in electric vertical take-off and landing vehicles are increasing attention on UAM for its potential to alleviate roadway traffic congestion. Given the spatial heterogeneity of land use in most cities, large-scale UAM will likely be deployed between specific urban areas, for example, from the suburbs to city centers. However, large-scale UAM travel between a few origin-destination pairs increases the risk of aircraft collisions and air traffic congestion, especially at airline intersections. To address this, this work proposes a hybrid framework of traffic simulation and management for large-scale UAM. The framework achieves an elegant trade-off between air traffic safety and efficiency by combining route guidance and collision avoidance for UAM aircraft. With a centralized strategy, route guidance provides system optimal paths (composed of waypoints) for aircraft, aiming to minimize total travel time. With a distributed strategy, collision avoidance generates trajectories between given waypoints, ensuring aircraft safety separation. To the best of our knowledge, this work is one of the first to introduce both dynamic route guidance and collision avoidance for UAM. The results highlight that the framework can effectively prevent air traffic congestion and provide flexible UAM operations, e.g., dynamic airspace access management. The proposed framework has demonstrated great potential for large-scale UAM simulation and management.

Keywords: Urban air mobility, Multi-agent systems, Collision avoidance, Air traffic congestion, Route guidance

1. Introduction

With network capacity approaching saturation, traffic congestion in metropolises becomes a recurrent puzzle. Recent advances in electric vertical take-off and landing vehicles (eVTOLs) are promoting the use of urban low-altitude airspace as a new traffic resource. Urban air mobility (UAM) has emerged and received considerable interest for its potential to provide point-to-point travel in congested cities. With the aid of ride-hailing apps like Lyft or Uber, UAM is promising to provide safe, clean, and affordable transport services for passengers and goods (Garrow et al., 2021), as evidenced by the test flights of full-size eVTOLs (Dietrich and Wulff, 2020). In the coming decade, the UAM market is estimated to expand rapidly and reach $32 billion globally (Grandl et al., 2018).

As the large-scale deployment of UAM approaches, we need to investigate: *(i) the traffic behavior of individual UAM aircraft*; and *(ii) the traffic scheme of collective UAM aircraft*. Advances in individual autonomy and intelligence will support more flexible UAM operations, which differ from the pre-planned routes and fixed schedules of conventional aviation. The explosion of UAM operations lifts air traffic efficiency to a level as important as air traffic safety. For safety, UAM operations focus on aircraft collision (or conflict) avoidance at the individual level. For efficiency, UAM operations emphasize air traffic congestion resolution at the system level.

*Corresponding author.
Email addresses: wengcq@mail2.sysu.edu.cn (Canqiang Weng), can-caesar.chen@connect.polyu.hk (Can Chen), pantl@pcl.ac.cn (Tianlu Pan), zhrenxin@mail.sysu.edu.cn (Renxin Zhong)

Collision avoidance is a widely discussed topic in multi-agent systems (composed of vehicles), where methods for terrestrial and aerial vehicles are compatible despite the difference in degrees of freedom. Various algorithms have been reported over the past few decades, see e.g., Huang et al. (2019); Yasin et al. (2020) and literature therein. Some representative works are summarized in Table 1. In general, there are two strategies for collision avoidance: centralized solutions and distributed solutions. In centralized solutions, a hypothetical manager receives all the information (e.g., agents' positions and velocities) and uses it to make decisions for all agents, see e.g., Bahabry et al. (2019); Tang et al. (2021). The manager's commands are assumed to be followed by all agents, without considering the uncertainty of pilot behavior. In distributed solutions, each agent receives limited information within its detection range and uses it to make decisions for itself, see e.g., Van Den Berg et al. (2011); Long et al. (2017). An agent may be able to perceive the decisions of other agents but cannot directly change their decisions. In this context, the centralized strategy implies global optimal but requires mass computation. While the distributed strategy implies local optimal but has advantages in computational efficiency.

Table 1: A brief survey of collision avoidance algorithms.

	Strategy	Scenario	Methodology	Objective (*minimize*)
Jose and Pratihar (2016)	Centralized	2D grid network	A* and GA[a]	Total time spent / fuel consumption
Xue and Do (2019)	Centralized	2D space without obstacle	MILP[b]	Deviation from the reference trajectory
Alrifaee et al. (2014)	Centralized	2D space with obstacle	MPC[c]	Deviation from the reference trajectory
Bahabry et al. (2019); Tang et al. (2021)	Centralized	3D airline network	MILP[b]	Total time spent / total flying cost
Yang and Wei (2020)	Distributed	2D space without obstacle	Game Theory[d]	Total time spent
Quan et al. (2021)	Distributed	3D space with obstacle	APF[e]	Deviation from the reference trajectory
Van Den Berg et al. (2011)	Distributed	2D/3D space with obstacle	VO[f]	Deviation from the reference velocity
Long et al. (2017)	Distributed	2D/3D space without obstacle	DNN[g]	—

[a] Genetic Algorithm
[b] Mixed Integer Linear Program
[c] Model Predictive Control
[d] Logit level-k model
[e] Artificial Potential Field
[f] Velocity Obstacles
[g] Deep Neural Network

In the early deployment of UAM, structured airspace is used to reduce the risk of aircraft collisions. The design concept of airspace structure is to separate aircraft with different properties (e.g., speed, direction, and level of autonomy) using airspace barriers. A comprehensive review of airspace structure designs is available in the work (Bauranov and Rakas, 2021). To be concise, we summarize some key points. (i) The airspace structures proposed in academia and industry can be roughly categorized into four concepts (see Figure 1) and their integration. For example, the multi-layer sky lanes design (proposed by Jang et al., 2017) and the multi-layer air corridors design (proposed by Bradford, 2020) integrate the concepts of layers and tubes. (ii) Less structured airspace allows aircraft to fly with more degrees of freedom, leading to higher traffic density. However, high-density aircraft flying freely along self-preferred (often direct) routes would increase the risk of traffic congestion.

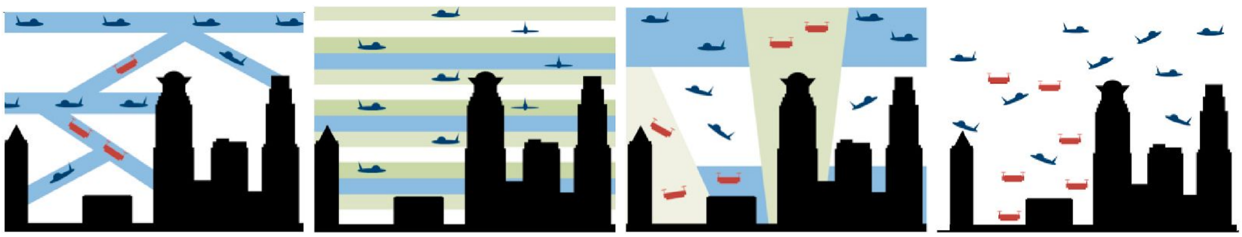

(a) Tubes (b) Layers (c) Zones (d) Full Mix

Figure 1: Different airspace structure designs for UAM, ordered by degrees of freedom (Sunil et al., 2015).

Although airspace structures provide a rule-based traffic scheme for UAM in its early stages, further investigation into air traffic management is needed to address future demands. Relevant studies in this area are being led by the US and Europe. NASA proposed the original concept of operations (ConOps) for unmanned aerial vehicle traffic management (UTM) in Kopardekar et al. (2016). Similarly, the European version of UTM, known as urban space (U-space), was proposed in Undertaking et al. (2017). A detailed discussion and comparison of the UTM and U-space ConOps can be found in Shrestha et al. (2021). The proposed ConOps is a type of guidelines that explain the functions of each part of the system and how they work together. Under the current UTM architecture, point-to-point operations relying on human operators have limitations on deployment scale. However, both UTM and U-space envision a future of large-scale UAM services with high-level autonomy. In this context, air traffic congestion caused by high-density UAM aircraft attracts more and more attention. Cummings and Mahmassani (2021) simulated point-to-point UAM operations in 3D space using a decentralized conflict resolution. Their simulations indicate that UAM faces similar congestion issues similar to roadway traffic. Safadi et al. (2023a) expanded the simulation scale and obtained complete relationships between air traffic flow, density, and speed. The air traffic flow is observed as a concave curve with respect to air traffic density, where the critical density provides a benchmark for identifying air traffic congestion (Cummings and Mahmassani, 2024). Based on the flow-density relationship, also known as the Macroscopic Fundamental Diagram (MFD), a few approaches have been proposed to manage air traffic congestion (see e.g., Haddad et al., 2021; Safadi et al., 2023b). Remarkably, the MFD framework implicitly assumes that traffic congestion is evenly distributed, i.e. the areas with an MFD should be (roughly) homogeneously loaded (Geroliminis and Sun, 2011). As a result, the origin-destination (OD) is set to be uniformly distributed in most current studies (Haddad et al., 2021; Safadi et al., 2024). However, it is hard to construct a uniformly distributed vertiport network [1] for UAM in practice, as land use in most cities is spatially heterogeneous (Wu and Zhang, 2021). UAM traffic is more likely to transfer between a few urban areas, for example, from the suburbs to city centers. The difference in air traffic operations between homogeneous and heterogeneous demand, as illustrated in Figure 2, has not received attention in studies.

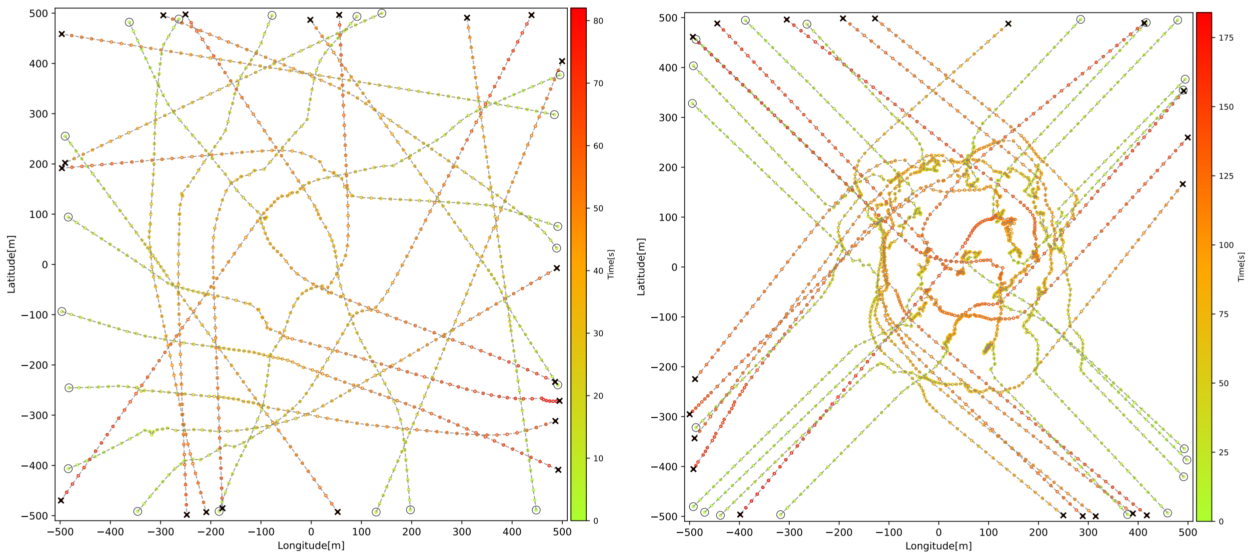

(a) Uniformly distributed OD

(b) Directionally distributed OD

Figure 2: Collision-free aircraft trajectories in 2D space with a deployment scale of 20, where 'O' marks the origin and 'X' marks the destination. Compared to homogeneous OD in (a), heterogeneous OD in (b) poses higher risks of delay and congestion.

To fill the above research gaps, we propose a hybrid framework of traffic simulation and management for large-scale UAM, as illustrated in Figure 3. The main contributions of this paper are summarized as follows:

1. The proposed framework is one of the first to combine route guidance and collision avoidance in the context of UAM, as far as we know. Route guidance provides time-efficient paths (composed of waypoints) for aircraft, while collision avoidance generates safe trajectories between given waypoints. In this way, the framework achieves an elegant trade-off between air traffic safety and efficiency.

[1]The vertiport network, which is regarded as the OD of air traffic in this paper, is the infrastructure for UAM aircraft to take off and land.

2. The proposed framework is efficient and flexible for large-scale UAM simulation and management. With a centralized strategy, route guidance dynamically regulates the spatial distribution of aircraft based on management purposes. With a distributed strategy, collision avoidance is accelerated by parallel computation. The results highlight some key points that the framework can (i) ensure air traffic homogeneity regardless of demand and (ii) provide dynamic airspace access management.

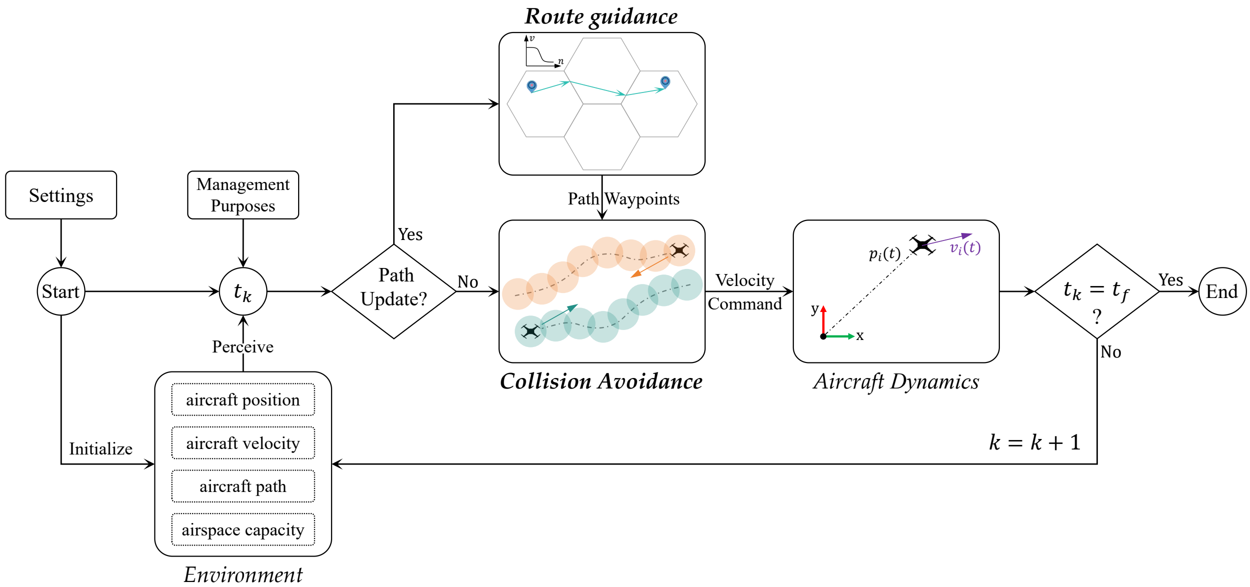

Figure 3: The hybrid framework for large-scale UAM simulation and management.

2. Methodology

The workflow of the proposed framework is illustrated in Figure 3 as follows. First, settings of airspace (e.g., region division), aircraft (e.g., safety radius, maximum speed), and UAM demand (e.g., aircraft ODs, departure ratio) are input to initialize the environment. Next, necessary information (e.g., aircraft position, velocity) is collected from the environment to assist in decision-making at each time step t_k. The decision-making process consists of two modules: route guidance and collision avoidance. At each time step t_k, the route guidance module updates paths for all aircraft if necessary, which will be detailed in subsection 2.2. Otherwise, the paths[2] remain consistent with those from the previous time step t_{k-1}. Here an aircraft's path refers to a sequence of waypoints corresponding to the airspace region division. Based on the path decision, the collision avoidance module generates velocity commands to guide aircraft to travel between waypoints, which will be detailed in subsection 2.1. Lastly, the decision-making process is repeated over time until the mission is complete (i.e, $t_k = t_f$).

2.1. Collision avoidance

In this section, we introduce the collision avoidance module of the proposed framework. We achieve collision avoidance for 3D aircraft motion using the velocity obstacles model. At each time step t_k, the position and velocity of an aircraft $A_i \in \mathbb{U}_A$ are denoted by $\mathbf{p}_i(t_k) \in \mathbb{R}^3$ and $\mathbf{v}_i(t_k) \in \mathbb{R}^3$, respectively. For aircraft discussed in this paper, we suppose the following dynamics are satisfied

$$\mathbf{p}_i(t_{k+1}) = \mathbf{p}_i(t_k) + \mathbf{v}_i(t_k)\Delta t \tag{1a}$$
$$\mathbf{v}_i(t_k) = \mathbf{v}_i^c(t_k) \tag{1b}$$

[2]The initial path of each aircraft is a direct route from origin to destination.

where Δt is the simulation time and $\mathbf{v}_i^c(t_k)$ is the velocity command.

The velocity command $\mathbf{v}_i^c(t_k)$ is generated using the *optimal reciprocal collision avoidance* (ORCA) method, referring to Van Den Berg et al. (2011). Concretely, the velocity command $\mathbf{v}_i^c(t_k)$ is chosen from the permitted velocities to be as close as possible to its preferred velocity [3] $\mathbf{v}_i^p(t_k)$, i.e.,

$$\mathbf{v}_i^c(t_k) = \underset{\mathbf{v} \in ORCA_A^\tau}{\arg\min} \|\mathbf{v} - \mathbf{v}_i^p(t_k)\| \tag{2}$$

where $ORCA_A^\tau$ is the set of permitted velocities that enables aircraft A_i to avoid collisions with other aircraft during the time horizon τ. The permitted velocities of aircraft A_i are influenced by all aircraft within the detection range, i.e.,

$$ORCA_A^\tau = \bigcap_{A_j \in \mathbb{N}_i} ORCA_{A_i|A_j}^\tau \tag{3}$$

where $\mathbb{N}_i$ is the set of aircraft within the detection range of aircraft A_i and $ORCA_{A_i|A_j}^\tau$ is the permitted velocities of aircraft A_i induced by aircraft A_j. The set of $ORCA_{A_i|A_j}^\tau$ depends on the relative position and velocity between aircraft A_i and A_j. To keep this paper concise, we suggest readers refer to Van Den Berg et al. (2011) for details on the ORCA method.

2.2. Route guidance

In this section, we introduce the route guidance module of the proposed framework. To provide a map for aircraft routing, we divide the airspace into several non-overlapping regions, denoted by $R_l \in \mathbb{U}_R$. Inspired by cellular communications, the airspace regions are designed as hexagons. Given an aircraft position $\mathbf{p} \in \mathbb{R}^3$, we introduce an indicator function

$$\Phi(\mathbf{p}, R_l) = \begin{cases} 1, & \text{if } \mathbf{p} \in R_l \\ 0, & \text{else} \end{cases} \tag{4}$$

to declare whether the aircraft is within the airspace region. Thus the aircraft accumulation in airspace region R_l can be calculated as follows

$$n_l(t) = \sum_{A_i \in \mathbb{U}_A} \Phi(\mathbf{p}_i(t), R_l) \tag{5}$$

To capture the influence of airspace traffic congestion, we suppose that the travel speed within airspace region R_l satisfies

$$V_{R_l}(t) = \frac{\exp\left(n_l^{cr} - n_l(t)\right)}{1 + \exp\left(n_l^{cr} - n_l(t)\right)} V_{R_l}^{max} \tag{6}$$

where n_l^{cr} and $V_{R_l}^{max}$ represent the critical accumulation and maximum travel speed of airspace region R_l, respectively. The travel speed within an airspace region will decrease as the aircraft accumulation increases. As a result, the travel time spent will increase as traffic congestion increases and we have

$$\int_t^{t+T_{R_l}} V_{R_l}(s) ds = D_l \tag{7}$$

where T_{R_l} and D_l are the travel time spent and average travel distance in airspace region R_l, respectively.

To formulate the route guidance problem, we represent an aircraft's path as $P_i \in \mathcal{P}_i$, where $\mathcal{P}_i$ denotes the set of permitted paths for aircraft A_i to travel from its origin to destination. We consider path P_i travel in several airspace regions. Then the travel time spent on path P_i is derived as follows

$$T_i(P_i) = \sum_{R_l \in P_i} T_{R_l} \tag{8}$$

The route guidance is designed to find optimal paths for all aircraft to minimize the total travel time spent, i.e.,

$$\min_{P_i \in \mathcal{P}_i} \sum_{A_i \in \mathbb{U}_A} T_i(P_i) \tag{9}$$

[3] The preferred velocity of an aircraft is typically directed towards its destination (the current waypoint).

3. Results

To evaluate the performance of the proposed framework, we design a baseline for comparison. The baseline employs air corridors for air traffic management (Jang et al., 2017; Kopardekar et al., 2016), where aircraft travel within predefined air corridors and avoid collisions using the method [4] in subsection 2.1. The baseline management scheme is tested in different scenarios for a comprehensive investigation, as illustrated in Figure 4. For each scenario, we provide tests in 2D space (at a fixed altitude of 500m) and 3D space (within altitude ranges of 450-550m and 400-600m).

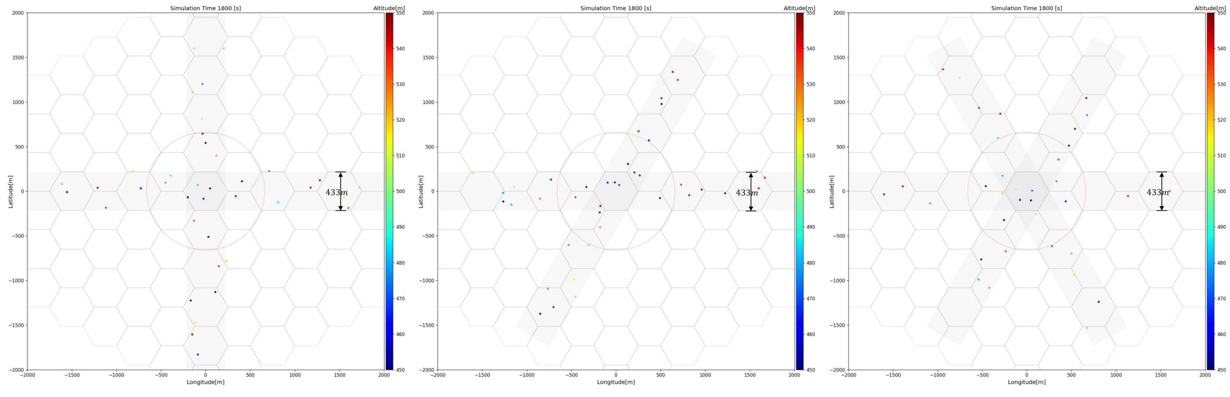

(a) "+" type (b) "#" type (c) "∗" type

Figure 4: Test scenarios: (a) two orthogonal air corridors intersecting; (b) two oblique air corridors intersecting; (c) three air corridors intersecting.

As the altitude range increases, the capacity of air corridors to handle UAM demand will also increase. Thus the aircraft inflows are set differently, see Figure 5. Considering different scenarios and altitude ranges, we conducted 9 tests for the baseline scheme, with each test repeated 5 times. Intuitive results are shown in Figure 10a, Figure 10c and Figure 10e. A qualitative finding is that air traffic congestion tends to occur and spread from the corridor intersections, regardless of the way of corridor intersects. To provide quantitative insights, we measure traffic outflow and accumulation at the corridor intersections (marked by red circles in Figure 4). The results are illustrated in Figure 6, Figure 7 and Figure 8. The traffic outflow-accumulation relationship is observed to be concave with a single peak, where air traffic evolves from free-flow states to critical states and eventually to congestion states. Referring to Haddad et al. (2021), we fit the MFD curve in the form of $G(N) = \alpha N \exp\big(-\frac{1}{\beta}(\frac{N}{N^{cr}})^{\beta}\big)$. It is easy to find that the critical points (marked by 'Δ') of MFD curves are significantly influenced by the permitted altitude range of aircraft rather than the way of corridor intersects. In other words, the capacity of the given airspace depends on its volume.

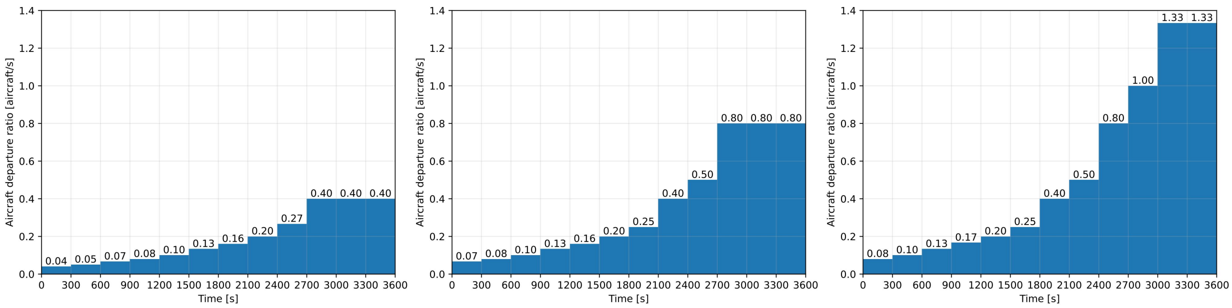

(a) (b) (c)

Figure 5: Aircraft inflow patterns for different tests: (a) $z = 500m$; (b) $z \in [450, 550]m$; (c) $z \in [400, 600]m$, where z denotes aircraft altitude.

[4]The aircraft settings are as follows: detection radius $r_d = 200m$, safety radius $r_s = 50m$, maximum speed $v^{max} = 20m/s$

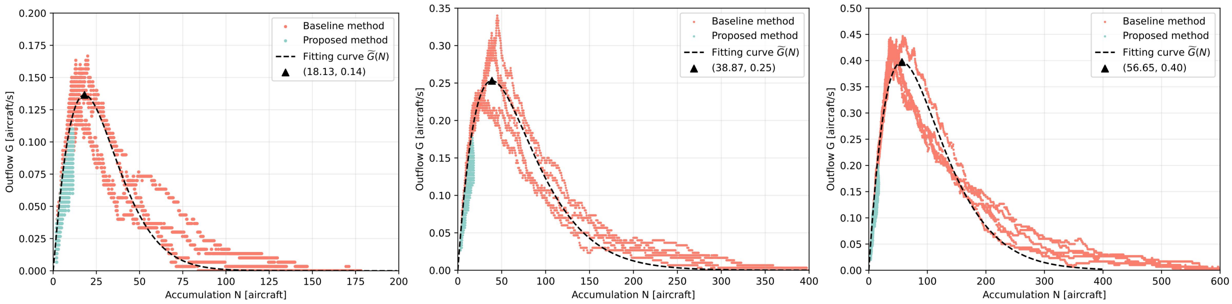

(a) $z = 500m$ (b) $z \in [450, 550]m$ (c) $z \in [400, 600]m$

Figure 6: The simulation results of outflow-accumulation relationships in the "+" type scenario.

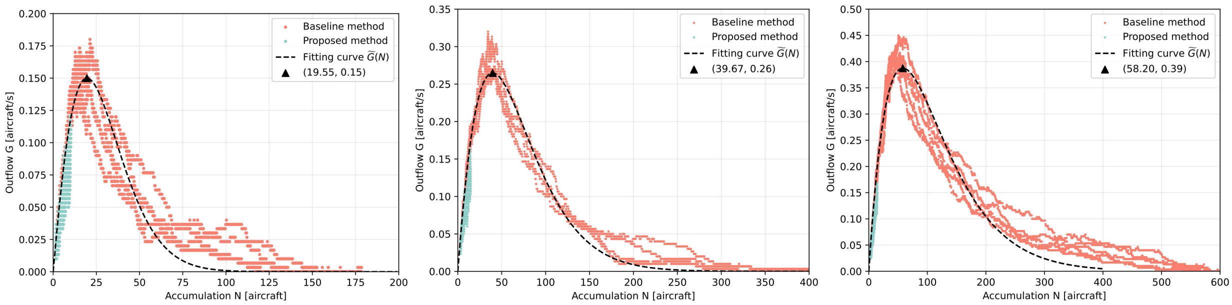

(a) $z = 500m$ (b) $z \in [450, 550]m$ (c) $z \in [400, 600]m$

Figure 7: The simulation results of outflow-accumulation relationships in the "#" type scenario.

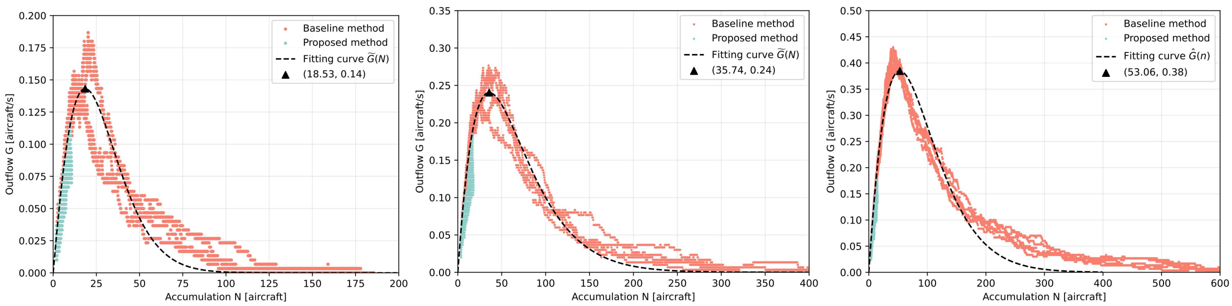

(a) $z = 500m$ (b) $z \in [450, 550]m$ (c) $z \in [400, 600]m$

Figure 8: The simulation results of outflow-accumulation relationships in the "∗" type scenario.

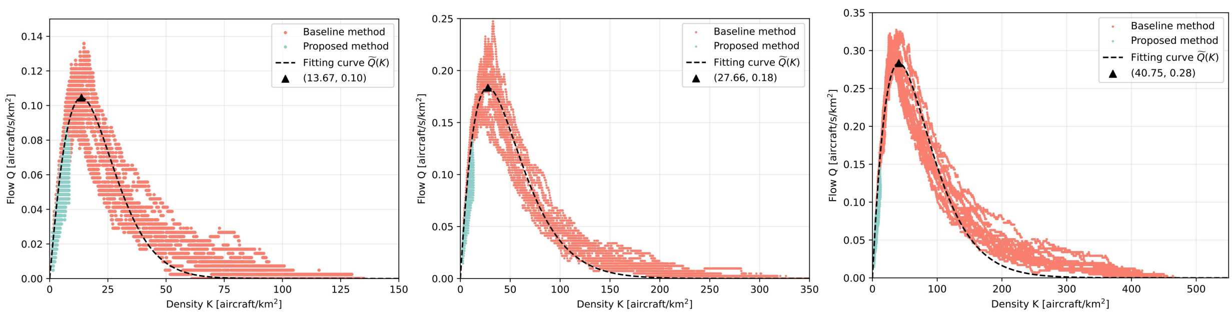

(a) $z = 500m$ (b) $z \in [450, 550]m$ (c) $z \in [400, 600]m$

Figure 9: The simulation results of flow-density relationships.

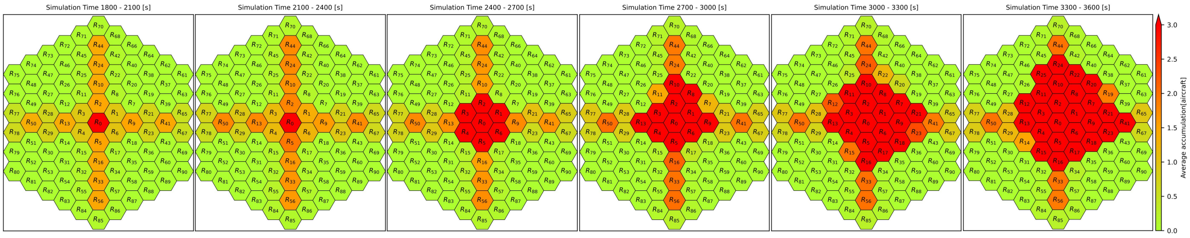

(a) The results of the baseline method in "+" type scenario.

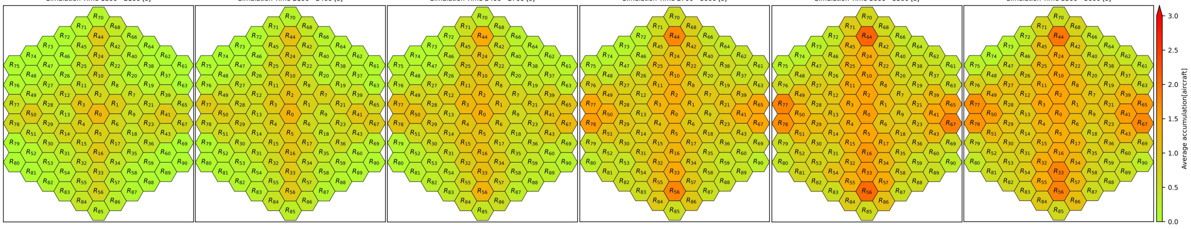

(b) The results of the proposed method in "+" type scenario.

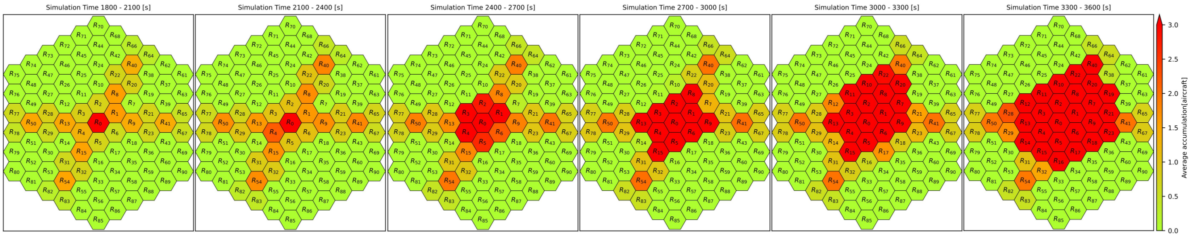

(c) The results of the baseline method in "#" type scenario.

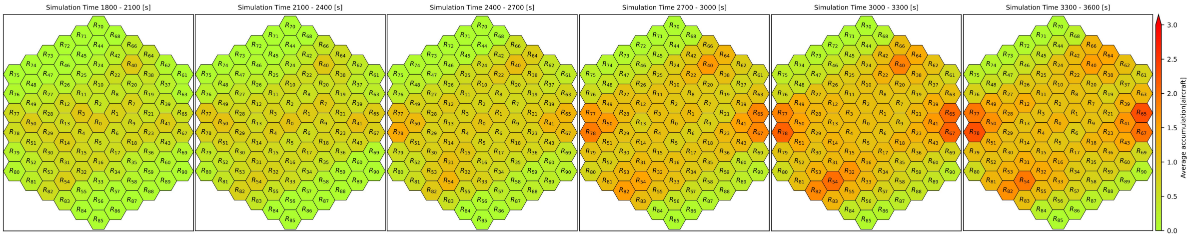

(d) The results of the proposed method in "#" type scenario.

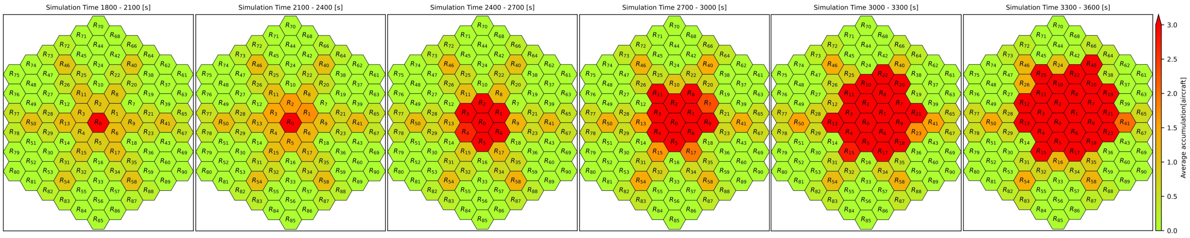

(e) The results of the baseline method in "$*$" type scenario.

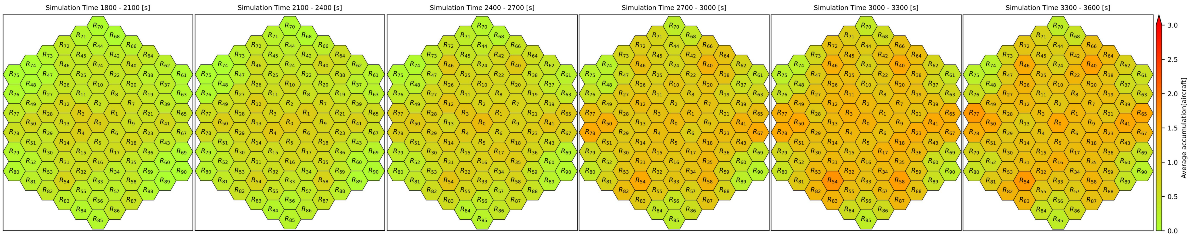

(f) The results of the proposed method in "$*$" type scenario.

Figure 10: The airspace traffic state evolution comparison.

To calibrate airspace capacity, we aggregate the results from different scenarios to obtain the relationship between airspace traffic flow and density, as illustrated in Figure 9. We provide a quantitative comparison of airspace capacity in Table 2. Remarkably, the calibration of the critical traffic accumulation (or density) is a necessary step for the route guidance module, see equation (6). Taking the baseline as a benchmark, we tested the proposed framework under the same simulation settings. Intuitive results are shown in Figure 10b, Figure 10d and Figure 10f. By introducing the mechanism of route guidance, the proposed framework can allocate aircraft uniformly into the available airspace. In this way, the proposed method effectively ensures traffic homogeneity, which is an implicit assumption of MFD frameworks (Geroliminis and Sun, 2011). Under the congested demand of the baseline, the proposed method effectively prevents air traffic deadlock at corridor intersections. Quantitative results are illustrated in Figure 6 - Figure 9 that air traffic remains in a free-flow state with the proposed method, bringing higher traffic safety and efficiency.

Table 2: The airspace capacity comparison.

	$\widetilde{K}_{jam}$ [aircraft/km^2]	$\widetilde{K}_{cr}$ [aircraft/km^2]	$\widetilde{Q}(\widetilde{K}_{cr})$ [aircraft/s/km^2]
Results with $z = 500$	75	13.67	0.10
Results with $z \in [450, 550]$	200	27.66 (102% ↑)	0.18 (80% ↑)
Results with $z \in [400, 600]$	300	40.75 (198% ↑)	0.28 (180% ↑)

Furthermore, the route guidance module of the proposed framework can provide flexible airspace management as needed. Note that a decrease in the capacity of an airspace region would restrict aircraft from entering that region, as discussed in subsection 2.2. Thus we can manage airspace access by region for various purposes, e.g., responding to emergencies. Figure 11 illustrates an example of airspace clearance induced by capacity regulation. The clearance in airspace region R_0, R_1 and R_4 is dynamic for $t \in [2400, 3000]s$, with tiny external impacts. The simulation results demonstrate the effectiveness of the proposed framework for large-scale UAM simulation and management.

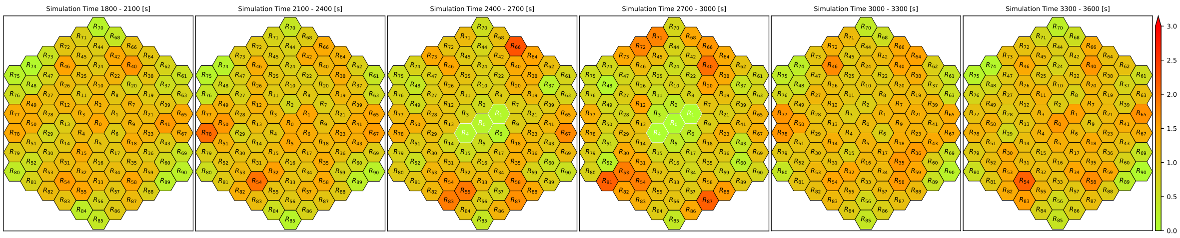

Figure 11: Dynamic airspace access management via capacity regulation: the airspace clearance of regions R_0, R_1, R_4 in $t \in [2400, 3000]s$ is generated for emergencies.

4. Conclusion

This paper focuses on traffic simulation and management for large-scale UAM. Considering the spatial heterogeneity of traffic demand, dense point-to-point UAM operations will increase the risk of aircraft collisions and air traffic congestion, especially at airline intersections. To address this, this work proposes a hybrid framework combining route guidance and collision avoidance for UAM aircraft. Route guidance provides time-efficient paths (composed of waypoints) for aircraft, while collision avoidance generates safe trajectories between given waypoints. In this way, the proposed framework achieves an elegant trade-off between air traffic safety and efficiency. The results highlight that the framework can effectively prevent air traffic congestion and provide flexible UAM operations, e.g., dynamic airspace access management. The proposed framework has demonstrated great potential for large-scale UAM simulation and management.

Acknowledgement

The work in this paper was supported by research grants from the National Natural Science Foundation of China (No. 72071214 & 62203239).

References

Alrifaee, B., Mamaghani, M.G., Abel, D., 2014. Centralized non-convex model predictive control for cooperative collision avoidance of networked vehicles, in: 2014 IEEE international symposium on intelligent control (ISIC), IEEE. pp. 1583–1588.

Bahabry, A., Wan, X., Ghazzai, H., Menouar, H., Vesonder, G., Massoud, Y., 2019. Low-altitude navigation for multi-rotor drones in urban areas. IEEE Access 7, 87716–87731.

Bauranov, A., Rakas, J., 2021. Designing airspace for urban air mobility: A review of concepts and approaches. Progress in Aerospace Sciences 125, 100726.

Bradford, S., 2020. Urban air mobility (uam) concept of operations. Federal Aviation Administration. .

Cummings, C., Mahmassani, H., 2021. Emergence of 4-d system fundamental diagram in urban air mobility traffic flow. Transportation Research Record 2675, 841–850.

Cummings, C., Mahmassani, H., 2024. Airspace congestion, flow relations, and 4-d fundamental diagrams for advanced urban air mobility. Transportation Research Part C: Emerging Technologies 159, 104467.

Dietrich, A., Wulff, Y., 2020. Urban air mobility: Adding the third dimension to urban and regional transportation, in: Presentation for: An Introduction to Urban Air Mobility for State and Local Decision Makers: A Virtual Workshop, sponsored by the Community Air Mobility Initiative (CAMI). Available online at https://www. communityairmobility. org/uam101.

Garrow, L.A., German, B.J., Leonard, C.E., et al., 2021. Urban air mobility: A comprehensive review and comparative analysis with autonomous and electric ground transportation for informing future research. Transportation Research Part C: Emerging Technologies 132, 103377.

Geroliminis, N., Sun, J., 2011. Properties of a well-defined macroscopic fundamental diagram for urban traffic. Transportation Research Part B: Methodological 45, 605–617.

Grandl, G., Ostgathe, M., Cachay, J., Doppler, S., Salib, J., Ross, H., 2018. The future of vertical mobility: A porsche consulting study.

Haddad, J., Mirkin, B., Assor, K., et al., 2021. Traffic flow modeling and feedback control for future low-altitude air city transport: An mfd-based approach. Transportation Research Part C: Emerging Technologies 133, 103380.

Huang, S., Teo, R.S.H., Tan, K.K., 2019. Collision avoidance of multi unmanned aerial vehicles: A review. Annual Reviews in Control 48, 147–164.

Jang, D.S., Ippolito, C.A., Sankararaman, S., Stepanyan, V., 2017. Concepts of airspace structures and system analysis for UAS traffic flows for urban areas, in: AIAA Information Systems-AIAA Infotech@ Aerospace, p. 0449.

Jose, K., Pratihar, D.K., 2016. Task allocation and collision-free path planning of centralized multi-robots system for industrial plant inspection using heuristic methods. Robotics and Autonomous Systems 80, 34–42.

Kopardekar, P., Rios, J., Prevot, T., Johnson, M., Jung, J., Robinson, J.E., 2016. Unmanned aircraft system traffic management (UTM) concept of operations, in: AIAA Aviation and Aeronautics Forum (Aviation 2016).

Long, P., Liu, W., Pan, J., 2017. Deep-learned collision avoidance policy for distributed multiagent navigation. IEEE Robotics and Automation Letters 2, 656–663.

Quan, Q., Fu, R., Cai, K.Y., 2021. Practical control for multicopters to avoid non-cooperative moving obstacles. IEEE Transactions on Intelligent Transportation Systems 23, 10839–10857.

Safadi, Y., Fu, R., Quan, Q., Haddad, J., 2023a. Macroscopic fundamental diagrams for low-altitude air city transport. Transportation Research Part C: Emerging Technologies 152, 104141.

Safadi, Y., Geroliminis, N., Haddad, J., 2024. Integrated departure and boundary control for low-altitude air city transport systems. Transportation Research Part B: Methodological , 103020.

Safadi, Y., Geroliminis, N., Haddad, J., et al., 2023b. Aircraft departures management for low altitude air city transport based on macroscopic fundamental diagram, in: 2023 American Control Conference (ACC), IEEE. pp. 4393–4398.

Shrestha, R., Oh, I., Kim, S., et al., 2021. A survey on operation concept, advancements, and challenging issues of urban air traffic management. Frontiers in Future Transportation 2, 626935.

Sunil, E., Hoekstra, J., Ellerbroek, J., Bussink, F., Nieuwenhuisen, D., Vidosavljevic, A., Kern, S., 2015. Metropolis: Relating airspace structure and capacity for extreme traffic densities, in: ATM seminar 2015, 11th USA/EUROPE Air Traffic Management R&D Seminar.

Tang, H., Zhang, Y., Mohmoodian, V., Charkhgard, H., 2021. Automated flight planning of high-density urban air mobility. Transportation Research Part C: Emerging Technologies 131, 103324.

Undertaking, S.J., et al., 2017. U-space: blueprint. .

Van Den Berg, J., Guy, S.J., Lin, M., Manocha, D., 2011. Reciprocal n-body collision avoidance, in: Robotics Research: The 14th International Symposium ISRR, Springer. pp. 3–19.

Wu, Z., Zhang, Y., 2021. Integrated network design and demand forecast for on-demand urban air mobility. Engineering 7, 473–487.

Xue, M., Do, M., 2019. Scenario complexity for unmanned aircraft system traffic, in: AIAA Aviation 2019 Forum, p. 3513.

Yang, X., Wei, P., 2020. Scalable multi-agent computational guidance with separation assurance for autonomous urban air mobility. Journal of Guidance, Control, and Dynamics 43, 1473–1486.

Yasin, J.N., Mohamed, S.A., Haghbayan, M.H., Heikkonen, J., Tenhunen, H., Plosila, J., 2020. Unmanned aerial vehicles (uavs): Collision avoidance systems and approaches. IEEE access 8, 105139–105155.